

GAS FLOW IN NANOSCALE DEVICES

ABSTRACT:

The flow of gases in nanoscale devices is examined. It is shown that conventional analysis methods, such as the Navier-Stokes equation, cannot be used at such small scales. An equation that is valid for all scales of flow, the Boltzman equation, is derived from the Liouville equation. Two mesoscopic solvent models, direct simulation Monte Carlo and stochastic rotational dynamics, as well as a higher order continuum equation, the Burnett equation are also introduced. Applications of these equations are considered, and their results are compared to experimental data, and each other.

SECTION 1: INTRODUCTION

Nanoscale fluidic devices are a burgeoning technology, with the potential for great scientific discovery as well as industrial applications. While most of these devices are geared towards the transport of liquids, there are many applications for gas transporting devices, these applications include the design of heat sinks, catalyst particles and filters with monodisperse pore sizes.

The theory that describes how these devices works is in its infancy. However, the devices themselves have proliferated rapidly primarily due to the use of lithographic techniques used for patterning semiconductor chips for the electronics industry. These techniques have been used to create nanoscopic channels in monocrystalline silicon [1] and glass [2]. However, these techniques produce channels that are either rectangular, trapezoidal or hexagonal in cross-section rather than circular [1,3,4,5]. This adds complexity to the analysis of flow but it is beyond the scope of this paper. The size of these channels can vary in diameter from 100 μm to 0.1 nm.

Typically, the Navier-Stokes (NS) equation is used to describe the behavior of fluids. However, this equation assumes that the density, the momentum and the temperature are smooth continuous functions. Fluids are discrete in nature, and when the distance between particles is

significant relative to the size of the system, the continuity assumption collapses. The discreteness of a fluidic system is characterized by the Knudsen number, Kn . Kn is the ratio of the mean free path length to the characteristic length of the system. If $Kn < 0.1$ [6], the Navier-Stokes equation can be used. If Kn is > 0.1 , then the flow must be analyzed by different methods.

For all values of Kn , the behaviour of the fluid can be calculated by directly integrating the equations of motion for the individual particles, subject to the appropriate forces and boundary conditions. This process, typically referred to as a molecular dynamics simulation, is extremely computationally intensive. Approximations have been made to simplify these simulations. The most common approximation, a simplification to the particle collision rule, leads to the Boltzmann Equation (B). Unfortunately, because of the computational requirements of the B equation, it is seldom possible to simulate these systems for more than a few picoseconds, while most flow behaviour cannot be determined without microseconds of simulation [7]. It is possible to make even further simplifications to the B equation. Within a diminished range of Kn , the results of these simplifications result in meso-scopic solvent models, such as direct simulation monte carlo (DSMC) and stochastic rotation dynamics (SRD), and higher order continuum equations such as the Burnett equation. In general: for $Kn < 0.1$, the NS equation is used; for $0.1 < Kn < 10$, the meso-scopic solvent models are used; and for $Kn > 10$, the B equation is used [6].

The rest of this paper will be divided as follows. Sections 2-5 will introduce the equations and explain their principles of operation, Section 6 will provide examples of applications of these equations and when possible connect them to experimental evidence. Finally, section 7 will summarize the results of this paper.

SECTION 2: THE BOLTZMAN EQUATION:

To derive the hydrodynamic properties, we are interested in the average properties of a single particle [8, 9]. Consider an equilibrium system of N particles with Hamiltonian $H(\vec{r}^N, \vec{p}^N)$. The probability of all the particles having a specified set of positions and momenta (phase point) is given by a phase-space probability density $f^{(N)}(\vec{r}^N, \vec{p}^N, t)$. The time evolution of this probability density is given by Liouville equation,

$$\frac{\partial f^{(N)}}{\partial t} = -L f^{(N)} \quad 2.1$$

where L is the Liouville operator,

$$L = \sum_{i=1}^{3N} \left(\frac{\partial H}{\partial r_i} \frac{\partial}{\partial p_i} - \frac{\partial H}{\partial p_i} \frac{\partial}{\partial r_i} \right) \quad 2.2$$

It can be shown that all the equations used to analyze flow can be derived from the Liouville equation. While this is useful, it does not provide assistance in determining the behaviour of a single particle in the system. A reduced phase space probability density function $f^{(n)}(\vec{r}^n, \vec{p}^n, t)$ can be defined that specifies the phase space behaviour of n of the N particles of the system,

$$f^{(n)}(\vec{r}^n, \vec{p}^n, t) = \frac{N!}{(N-n)!} \iint f^{(N)}(\vec{r}^N, \vec{p}^N, t) d\vec{r}^{(N-n)} d\vec{p}^{(N-n)} \quad 2.3$$

The time evolution of this probability density is considerably more complicated. In general, a recurrence relationship can be found of the form,

$$\frac{\partial f^{(n)}}{\partial t} + \frac{1}{m} \sum_{i=1}^n \vec{p}_i \cdot \frac{\partial f^{(n)}}{\partial \vec{r}_i} + \sum_{i=1}^n \vec{F}_i \cdot \frac{\partial f^{(n)}}{\partial \vec{p}_i} = - \sum_{i=1}^n \sum_{j=1}^n \Psi_{ij} \cdot \frac{\partial}{\partial \vec{p}_i} - \sum_{i=1}^n \iint \Psi_{i(n+1)} \cdot \frac{\partial}{\partial \vec{p}_i} f^{(n+1)} d\vec{r}_{n+1} d\vec{p}_{n+1} \quad 2.4$$

where \vec{F}_i is an external force acting on the i^{th} particle, and Ψ_{ij} is the interaction force between particles i and j.

In order to calculate the trajectory of a single particle in a system, the reduced distribution function of a single particle must be calculated. Thus equation 2.4 becomes,

$$\left(\frac{\partial}{\partial t} + \frac{1}{m} \sum_{i=1}^3 p_i \cdot \frac{\partial}{\partial r_i} + \sum_{i=1}^3 F_{vi} \cdot \frac{\partial}{\partial p_i} \right) f^{(1)}(\vec{r}_1, \vec{p}_1, t) = - \iint \Psi_{12} \cdot \frac{\partial}{\partial \vec{p}_1} f^{(2)}(\vec{r}_1, \vec{p}_1, \vec{r}_2, \vec{p}_2, t) d\vec{r}_2 d\vec{p}_2 \quad 2.5$$

Under the assumptions that collisions between particles are binary in nature (i.e. no more than two particles collide at any time) and that successive collisions are uncorrelated, Boltzman simplified equation 2.5 to,

$$\left(\frac{\partial}{\partial t} + \frac{1}{m} \sum_{i=1}^3 p_i \cdot \frac{\partial}{\partial r_i} + \sum_{i=1}^3 F_{vi} \cdot \frac{\partial}{\partial p_i} \right) f^{(1)}(\vec{r}_1, \vec{p}_1, t) = \left(\frac{\partial f^{(1)}}{\partial t} \right)_{collisions} \quad 2.6$$

Where the right hand term is,

$$\left(\frac{\partial f^{(1)}}{\partial t} \right)_{collisions} = \frac{1}{m} \sum_{i=2}^N \iint \sigma(\Omega, |\vec{p}_1 - \vec{p}_2|) |\vec{p}_1 - \vec{p}_2| \left[f^{(1)}(\vec{r}_1, \vec{p}'_1, t) f^{(1)}(\vec{r}_1, \vec{p}'_2, t) - f^{(1)}(\vec{r}_1, \vec{p}_1, t) f^{(1)}(\vec{r}_1, \vec{p}_2, t) \right] d\Omega d\vec{p}_i$$

Here the primes denote post collision momenta and $\sigma(\Omega, |\vec{p}_1 - \vec{p}_2|)$ is the cross-section for scattering into a solid angle Ω , the simplest expression for this is $2\pi\Omega$ [9].

Equation 2.6 is the Boltzman kinetic equation. The advantage of this equation is that it is accurate for all Knudsen numbers. However, this too is computationally intensive. Integration of this equation for a low density system of particles, subject to the necessary constraints to maintain flow, will result in an accurate simulation of flow. Certain statistical averages of Hydrodynamic parameters can be used to calculate velocity profiles, pressure drops, viscosity coefficients and other rheological parameters. Let ψ_i be an observable flux associated with a particle of the system (e.g. $\psi_i = m_i \int f_i^{(1)} \vec{v}_i dv_i = j_i$ where j_i is the mass flux,

$$\psi_i = m_i \int v_{ix} f_i^{(1)} \vec{v}_i dv_i = \rho_i m_i \overline{v_{ix} \vec{v}_i} \text{ where this is the momentum flux in the x direction and}$$

$$\psi_i = \frac{m_i}{2} \int v_i^2 f_i^{(1)} \vec{v}_i dv_i = \frac{\rho_i m_i \overline{v_i^2 \vec{v}_i}}{2} \text{ where this is the energy flux) in general one can write the time}$$

evolution of ψ_i as [9],

$$\frac{\partial}{\partial t} \sum_i (\rho_i \overline{\psi_i}) + \nabla_r \cdot \sum_i (\rho_i \overline{\psi_i \vec{v}_i}) - \sum_i \rho_i \left\{ \frac{\partial \overline{\psi_i}}{\partial t} + \overline{v_i \cdot \nabla_r \psi_i} + \frac{\vec{F}_i}{m} \cdot \overline{\nabla_r \psi_i} \right\} = 0 \quad 2.7$$

Substituting the appropriate ψ_i recovers the continuity equation, the conservation of momentum equation and the conservation of kinetic energy equations that are required to derive the Navier-Stokes equation.

While the Boltzman equation establishes the time progression of the reduced phase-space density function, how does one establish that it does this in a physically realistic manner? For this, it is required that the Boltzman equation, or any other kinetic equation, satisfy two conditions; Boltzman invariance and Galilean invariance. The former is a statistical statement of the second law of thermodynamics which states that, as time progresses, the system progresses towards equilibrium. Galilean invariance requires that under any inertial frame of reference, the laws of motion remain unchanged. To prove the former, Boltzman established an H-theorem [9],

$$H(t) = \iint f(\vec{r}, \vec{v}, t) \ln f(\vec{r}, \vec{v}, t) d\vec{r} d\vec{v} \quad 2.8$$

Where $H(t)$ is analogous to entropy, hence requiring that $\frac{\partial H(t)}{\partial t} \leq 0$ for all t is analogous to

requiring that $\frac{\partial S(t)}{\partial t} \leq 0$ and the system will progress towards equilibrium. Galilean invariance is

satisfied as long as, for a collision, the probability of a particle being deflected by an angle θ is the same as the probability of a particle being deflected by an angle $-\theta$.

SECTION 3: THE NAVIER-STOKES EQUATION

In section 2, it was mentioned that different choices of ψ_i in equation 2.7 will produce the continuity equations we require for the Navier-Stokes equation. The resulting equations for conservation of mass, the continuity equation, and momentum in a differential element of fluid are [9, 10]:

$$\text{for mass, } \nabla \rho(\vec{v} \cdot \vec{n}) + \frac{\partial \rho}{\partial t} = 0 \quad 3.1$$

$$\text{for momentum, } \frac{\partial(\rho \bar{v}_x)}{\partial x} + \frac{\partial(\rho \bar{v}_y)}{\partial y} + \frac{\partial(\rho \bar{v}_z)}{\partial z} + \frac{\partial(\rho \bar{v})}{\partial t} = \nabla \tau_{-x} + \nabla \tau_{-y} + \nabla \tau_{-z} - \nabla p + \rho \mathbf{g} \quad 3.2$$

Where ρ is the local density, \bar{v} is the local velocity and n is the normal vector to the differential fluid element, ∇p is the pressure gradient, g is the gravitational acceleration and

$$\nabla \tau_{-x} = \frac{\partial \tau_{xx}}{\partial x} + \frac{\partial \tau_{yx}}{\partial y} + \frac{\partial \tau_{zx}}{\partial z} \text{ where } \tau_{yx} \text{ is the stress on the surface normal to } y \text{ in the } x \text{ direction.}$$

The right hand side in the momentum equation is the resolution of the F_i terms in equation 2.7.

The continuity equation can be used to simplify the left hand side of the momentum equation. The resulting equation is,

$$\rho \frac{D\bar{v}}{Dt} = \nabla \tau_{-x} + \nabla \tau_{-y} + \nabla \tau_{-z} - \nabla p + \rho g \quad 3.3$$

Where $\frac{D}{Dt} = v_x \frac{\partial}{\partial x} + v_y \frac{\partial}{\partial y} + v_z \frac{\partial}{\partial z} + \frac{\partial}{\partial t}$. At this point, the Stokes' viscosity relation, $\tau_{xy} = \mu \frac{\partial v_y}{\partial x}$,

where μ is the viscosity coefficient, is typically inserted into equation 3.3. This yields the Navier-Stokes equation,

$$\rho \frac{D\bar{v}}{Dt} = \mu \nabla^2 \bar{v} - \nabla p + \rho g \quad 3.4$$

The Navier-Stokes equation is the most common, and simplest, equation used to describe flow. However, it is contingent on validity of the continuity equation, which requires a continuous density. For low Knudsen numbers the discrete nature of the density can no longer be ignored and the equation is no longer valid [11].

SECTION 4: CONTINUUM EQUATIONS

There are several possible modifications that can be made to the Navier-Stokes equation to enhance its performance. Most pertain to modifications of the Stokes' viscosity relation, but these do not extend the range of Kn for which the equation is accurate. The Navier-Stokes equation is based only on the mean values of the hydrodynamic parameters, and hence it is a first order equation. It is possible to make corrections to equation by including 2nd moment terms,

and higher. The Burnett equation, a second order equation, is the most commonly used higher order equation. This equation is the continuum approximation to the Boltzman equation through the Chapman-Enskog approximation [11]. Burnett's actual equation is too large to be included in this article. The equation and its derivation can be found in its entirety in the original paper [11]. This equation also includes heat transport terms, so it is often used when thermal effects are important. It should be noted that, while Burnett's equation is assumed valid within the Knudsen range of 0.1 to 10, it has never been formally proven to be accurate outside the range of the Navier-Stokes equation [12].

SECTION 5: STOCHASTIC EQUATIONS

The Burnett equation is a continuum approximation to the Boltzman equation. While this is one method to alleviate the computational intensity of the latter equation, another approach is to try to find shortcuts in the simulation procedure and approximations to the Boltzman equation that can be simulated with greater ease. Approaches of this kind have led to the development of two mesoscopic solvent techniques, direct simulation monte carlo (DSMC) and stochastic rotation dynamics (SRD).

Direct simulation monte carlo method was developed by Bird [13, 14], and can be outlined as follows:

1. The domain being considered for simulation is subdivided into cells.
2. The particles are positioned within the domain with their initial velocities and positions.
3. The particles are moved and their interactions with the boundaries are computed
4. The particles are indexed into their respective cells
5. Within each cell, a random number of particles are selected for collision and the collision is performed.
6. The flow properties are calculated and the results are outputted.

7. Until the simulation has ended the algorithm loops through steps 3-6.

Randomly assigning collisions, rather than calculating when particle trajectories collide, provides a substantial decrease in the amount of calculation that needs to be performed in the Boltzman Equation. It can also be shown that this equation has the same properties as the Boltzman equation [13], and is hence Boltzman invariant and Galilean invariant.

The second method to be outlined here is SRD [15, 16, 17, 18]. This method has some similarities with DSMC, but it forgoes collisions entirely. In this case a collision is replaced with a random rotation of the momenta of the particles. In effect, the same as if the particles collided elastically with a massive stationary object. SRD operates as follows:

1. The domain of the simulation is subdivided into cells of size L^3
2. The particles are positioned within the domain so that their initial velocities and positions satisfy initial conditions
3. The particles are moved and their interactions with the boundaries are computed
4. The particles are displaced in a random direction by a random distance between zero and L , by a displacement vector \vec{d} .
5. The average momentum of the particles in each cell is calculated
6. The momenta of the particles in the cells are rotated about the average momentum of the cell in a random direction (θ, ϕ) (where θ and ϕ are the latitude and the azimuth in spherical coordinates). The same rotation is applied to all the particles in the same cell, but a different rotation is chosen for each cell.
7. All of the particles are displaced by $-\vec{d}$.
8. The flow properties are calculated and the results are outputted.
9. Until the simulation has ended the algorithm loops through steps 3-8.

The displacement by \bar{d} may seem unnecessary, but it is required for Galilean invariance [17].

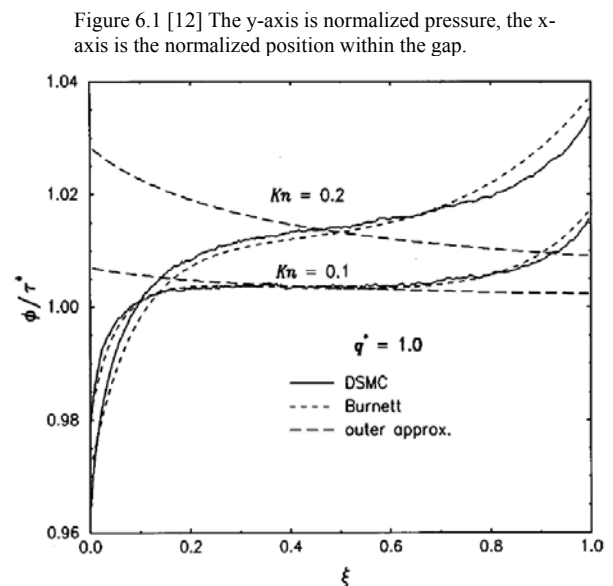
Despite the elimination of collisions the algorithm is also Boltzman invariant [15].

SECTION 6: EXPERIMENTAL RESULTS

As previously mentioned, the channels produced in nanofluidic devices have varying geometries. Hence simulations have been performed on channels of differing geometry. Because of the scale of the channels, measurements of flow parameters are difficult, and very few results have been published. Thus, it is difficult to find experimental data for which simulations of all kinds have been conducted and there is no common reference point.

As was mentioned in section 4, the Burnett equation includes thermal effects, it is frequently used to examine systems where thermal effects are important. An example of such a system was examined by Mackowski et al [12]. In this study, they created a system where a hard sphere potential gas was trapped between two plates separated by length L. A heat flux of q is induced between the two plates and maintained. Overtime, the system reaches steady state. The pressure distribution between the two plates is shown in figure 6.1 [12]. Note the strong agreement between the DSMC model and the Burnett equation. The outer equation is the result of expanding the Burnett equation solution to the normalized pressure in terms of Kn and truncating at Kn^2 .

For a rectangular channel, an approximate analytical solution to the NS equation is possible [14]. For a compressible fluid in a rectangular channel, with Kn dependent slip boundary conditions: The slip



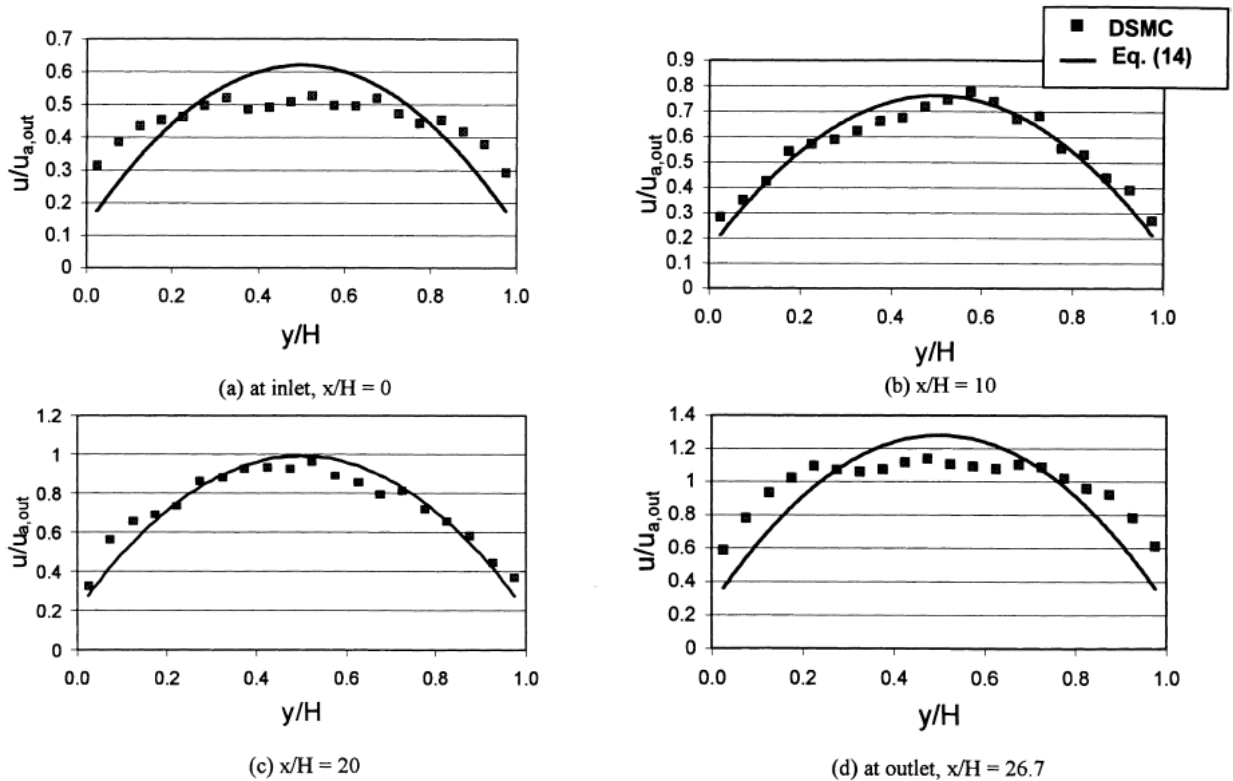
velocity is $u_{slip} = \frac{2-F}{F} Kn \frac{du}{dy} \Big|_{wall}$, where y is the channel width and F is the tangential

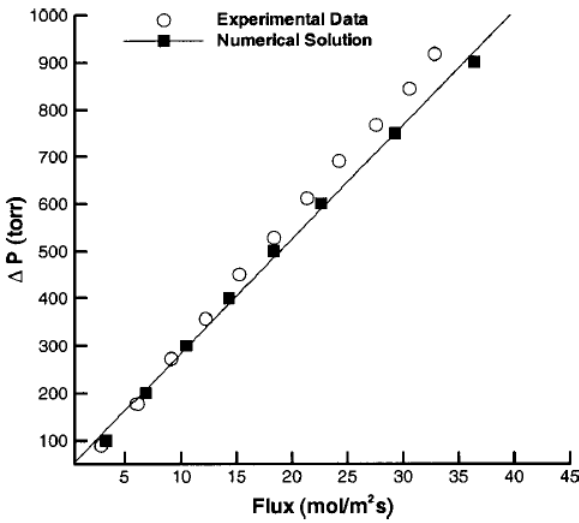
momentum accommodation coefficient. The steady state velocity profile, $u(x)$, along the length of the channel, x , is

$$u(x) = \frac{1}{2\mu} \frac{dp}{dx} \left(y^2 - \frac{H^2}{4} - \sigma H^2 Kn \right) \quad 6.1$$

where H is the channel height, μ is the viscosity coefficient and σ is $(2-F)/F$. The relationship between this projected velocity profile and the DSMC simulation of flow is shown below in figure 6.2. Experimental data on velocity profiles is very difficult to record for these devices. Pressure drop data is much easier to gather. Pressure drop data for argon gas across a membrane, containing 200nm cylindrical pores, is plotted vs. the predictions for the Navier-Stokes equation with slip flow boundary conditions in figure 6.3 [7].

Figure 6.2 [14]. Plots of normalized velocity, y -axis, vs. normalized position across the width of the channel, at different positions between the inlet and the outlet of the channel. Equation 14 is the same as equation 6.1.





L. Figure 6.3 [7] Pressure drop across a 200 nm pore membrane, vs. gas flux across the membrane.

R. Figure 6.4 [19] channel width vs. velocity, for $Kn = 1.84 \times 10^{-3}$, 2.32×10^{-2} and 4.64×10^{-2} .

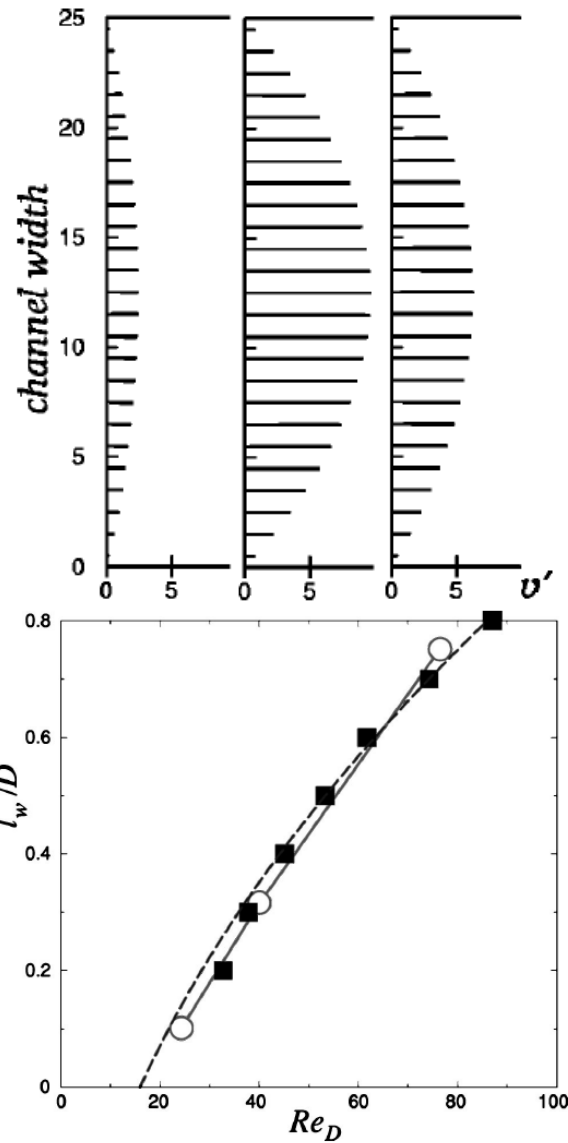


Figure 6.5 [19] Wake length behind a spherical obstacle in a channel vs. Reynolds number. Kn is proportional to Mach number over Reynolds number [7].

The SRD method has primarily been used to study flow in 2 dimensional systems. It has recently been extended to 3D applications [18, 19]. It has been used to study gravitational flow in channels of height H and infinite width, both an empty channel and a channel with a spherical barrier. Figure 6.4 [19] shows velocity profiles for an SRD model of flow in an empty channel, with a rotation angle of $\pm 90^\circ$, for Knudsen numbers of 1.84×10^{-3} , 0.0232×10^{-2} and 4.64×10^{-2} . The predictions of this model for flow around a spherical object are in good agreement with experimental measurements. Figure 6.5 shows a comparison of wake length vs. Reynolds number for experimental data and the SRD model [19].

SECTION 7: CONCLUSIONS

Partial differential equations are the basis for all analysis of fluid flow. In particular, the Liouville equation forms the basis for developing the Boltzman equation and from this equation

the Navier Stokes equation and Burnett equation are developed as well as the DSMC and SRD algorithms.

Fluid flow can be characterized by several equations of varying complexity, depending on the degree of accuracy needed in the description of the system. That degree of accuracy is dictated by the magnitude of fluctuations within the system, which is characterized by the ratio of the mean free path to the characteristic length of the system, or the Knudsen number. If $Kn < 0.1$, the NS equation is used for analysis. When $Kn > 10$, direct simulation of the B equation is the only method of analysis. The range of $0.1 < Kn < 10$ is a transition range where mesoscale solvent models like DSMC and SRD compete with higher order equations such as the Burnett equation.

While this intermediate range is of particular interest, there is very little experimental data within this range. Instead most systems for which there is data are with the range Kn which is still describable by the NS equation, and within the intermediate range. Equations such as the Burnett equation are typically compared to solvent models such as SRD and DSMC. The experimental data that does exist, confirms the accuracy of these models. Each of these models is suited to different tasks; SRD can very quickly analyze the behaviour of a gas. DSMC represents a more general version of SRD, which may not be as fast, but can analyze a larger variety of systems. Second order equations, such as Burnett equation, are capable of analyzing thermal effects on these solvents. If they are proven accurate, the latter may become the preferred form of analysis for these systems, as they can be solved using finite element methods. In the end, all of these equations have a vital role to play in expanding our understanding and design of nanofluidic devices.

SECTION 8: REFERENCES

- 1 Damean N, Regtien P P L (2001) Poiseuille Number for the Fully Developed Laminar Flow through Hexagonal Ducts Etched in $\langle 100 \rangle$ Silicon. *Sensors and Actuators A-Physical* **90** 96.
- 2 Harrison D J et al. (1993) Micromachining a Minaturized capillary electrophoresis-base. *Science* **261**(5123) 185.
- 3 Park S J et al. (2002) Modeling and Designing of Microfluidic System Using Poiseuille Number. 2nd Annual International IEEE-EMBS Special Topic Conference on Microtechnologies in Medicine and Biology 565.
- 4 Shah R K (1975) Laminar Flow Friction and Forced Convection Heat Transfer in Ducts of Arbitrary Geometry. *International Journal of Heat and Mass Transfer* **18** 849.
- 5 Weilin Q et al.(2000) Pressure Driven Water Flows in Trapezoidal Silicon Microchannels. *International Journal of Heat and Mass Transfer* **43** 353.
- 6 Jie D et al. (2000) Navier-Stokes Simulations of Gas Flow in Micro Devices. *Journal of Micromechanics and Microengineering* **10** 372.
- 7 Roy S et al. (2003) Modeling Gas Flow through Nano-Channels and Nano-Pores. *Journal of Applied Physics* **93**(8) 4870.
- 8 Hansen J P, McDonald I R. *Theory of Simple Liquids*. Academic Press, London UK 1986. pp. 13-17.
- 9 McQuarrie DA. *Statistical Mechanics*. University Science Books, Sausalito CA 2000. pp. 379-417.
- 10 Welty JR et al. *Fundamentals of Momentum, Heat and Mass Transfer-3rd edition*. John Wiley and Sons, Toronto ON 1984. pp. 120-128.
- 11 Burnett D (1935) The Distribution of Molecular Velocities and the Mean Motion in a Non-Uniform Gas. *Proceedings of the London Mathematical Society* **40** 382.
- 12 Mackowski D W et al. (1999) Comparison of Burnett and DSMC Predictions of Pressure Distributions and Normal Stress in One-Dimensional, Strongly Non-Isothermal Gasses. *Physics of Fluids* **11**(8) 2108.
- 13 Bird G A (1970) Direct Simulation and the Boltzman Equation. *The Physics of Fluids* **13**(11) 2676.
- 14 Xue H, et al. (2000) Prediction of Micro-Channel Flows Using Direct Simulation Monte Carlo. *Probabilistic Engineering Mechanics* **15** 213.
- 15 Malevanets A, Kapral R (1999) Mesoscopic Model for Solvent Dynamics. *Journal of Chemical Physics* **110**(17) 8605.
- 16 Malevanets A, Kapral R (2000) Solute Molecular Dynamics in a Mesoscale Solvent. *Journal of Chemical Physics* **112**(16) 7260.
- 17 Ihle T, Kroll D M (2003) Stochastic Rotation Dynamics. I. Formalism, Galilean Invariance, and Green-Kubo relations. *Physical Review E* **67** DOI 066705
- 18 Tüzel E et al. (2003) Stochastic Rotation Dynamics in Three Dimensions. *Physical Review E* **68** DOI 036701.
- 19 Allahyarov E, Gompper G (2002) Mesoscopic Solvent Simulations: Multiparticle Collision Dynamics of Three Dimensional Flows. *Physical Review E* **66** DOI 036702.

